A unified analytical solution for elastic-plastic stress analysis of a cylindrical cavity in Mohr-Coulomb materials under biaxial in-situ stresses

Pei-Zhi Zhuang*, Hai-Sui Yu

School of Civil Engineering, Faculty of Engineering,

University of Leeds, LS2 9JT Leeds, UK

* P.zhuang@leeds.ac.uk

ABSTRACT:

This paper presents a unified analytical solution for elastoplastic stress analysis around a cylindrical cavity under biaxial in-situ stresses during both loading and unloading. The two-dimensional solution is obtained by assuming that the connected plastic zone is statically determinate and using the complex variable theory in the elastic analysis. It is shown that the biaxial state of initial stresses applies significant influences on the stress distribution around the inner cavity. Under biaxial far-field stresses, the asymptotic conformal mapping function predicts that the outer boundary of the statically determinate plastic zone is in oval-shape in Mohr-Coulomb materials. The major axis of the elastic-plastic interface lies in the direction of the greatest far-field compression pressure during loading whereas it is along the perpendicular direction during unloading. The loading and unloading solutions are validated by comparing with numerical simulation results and other analytical solutions. In the assumed states, the new solution provides an accurate analytical method to capture the biaxial in-situ stress effect in the prediction of the plastic failure zone and calculations of the static stress field and the elastic displacement field around a cylindrical cavity within an infinite medium.

KEYWORDS:

K_0 effect, cavity expansion/contraction, complex variable theory, elastoplastic stress analysis

INTRODUCTION

Cylindrical cavity solutions have been applied in the analysis of a variety of geotechnical problems, for example, the expansion solutions provide a useful theoretical tool for estimating the maximum mud pressure during horizontal directional drillings (HDD) (Rostami et al., 2016, Staheli et al., 1998), the uplift resistance of strip anchors (Vesic, 1971, Yu, 2000), and the hydraulic fracturing pressure around a wellbore (Guo et al., 2015, Panah and Yanagisawa, 1989); the contraction solutions are commonly used in the stability analysis of tunnels or boreholes (Detournay and John, 1988, Mo and Yu, 2017, Yu and Rowe, 1999). In the analytical analysis, it is usually assumed that the cylindrical cavity is loaded or unloaded uniformly within a hydrostatic initial stress field. Thus the stress equilibrium and deformation compatibility conditions involved during expansions or contractions can be simply analysed as a one-dimensional axisymmetric problem (Bishop et al., 1945, Yu and Houlsby, 1991, 1995). In reality, however, the earth pressure at rest normally is non-hydrostatic, and a ratio of the horizontal to vertical effective soil stresses (i.e. earth pressure coefficient at rest, K_0) is often introduced to describe the in-situ stress state (Guo, 2010, Hu et al., 2017, Lee et al., 2013, Mayne and Kulhawy, 1982). Under biaxial far-field stresses, the stress distribution around a cavity may significantly differ from that computed in a simplified one-dimensional analysis (Bradford and Durban, 1998, Yarushina et al., 2010). Additional considerations of the K_0 effect may effectively further improve the accuracy of the cavity expansion/contraction theory in applications to the practical geotechnical problems, especially for horizontally excavated or buried structures at relatively shallow soil depths (Carranza-Torres and Fairhurst, 2000, Guo et al., 2015, Xia and Moore, 2006, Yanagisawa and Panah, 1994). Hence this note presents a unified analytical stress solution for both loading and unloading analysis of a cylindrical cavity considering the biaxial state of in-situ soil stresses.

Under non-hydrostatic far-field stresses, rigorous loading or unloading analysis of a cavity becomes more complicated, and, consequently, analytical solutions have been achieved only in a few cases such as in linear elastic materials (Muskhelishvili, 1963, Savin, 1970, Timoshenko and Goodier, 1951) and in power-law materials (Gao et al., 1991, Lee and Gong, 1987). Due to the high tendency to plastic yielding of soil even at relatively small strain levels, its response is more often characterized by non-linear constitutive models, for example, the commonly used elastic perfectly-plastic models.

Analytical solutions for the two-dimensional cylindrical cavity analysis in elastic perfectly-plastic materials was inspired primarily by the ingenious method developed by Galin (1946) in the loading analysis adopting the Tresca yield criterion, for example, the subsequent solutions considering various boundary conditions (Cherepanov, 1963, Parasyuk, 1948, Yarushina et al., 2010) and/or different materials (Detournay, 1986, Tokar, 1990).

In applications to geotechnical problems, the K_0 effect to the stress distribution around a cylindrical cavity during loading and unloading can be analytically investigated by the solutions of Galin (1946) and Yarushina et al. (2010) respectively, characterising the behaviour of undrained clay with the Tresca yield criterion. In more general cases of cohesive-frictional materials, an approximate analytical solution for the unloading stress analysis has been derived by Detournay and Fairhurst (1987) based on the Mohr-Coulomb yield criterion. However, analytical solutions considering biaxial far-field stresses for the loading analysis in Mohr-Coulomb materials have not been achieved yet. In addition, it has been pointed out that a stress discontinuity across the elastic-plastic interface exists in the unloading solution of Detournay and Fairhurst (1987). Hence, a new analytical solution for the two-dimensional stress analysis during loading is developed in this note, and the elastic complex potentials for the unloading analysis are also re-derived to eliminate the unnecessary stress discontinuity phenomenon.

PROBLEM DEFINITION AND BOUNDARY CONDITIONS

A cylindrical cavity embedded in a homogenous and isotropic infinite mass is considered as shown in Fig.1, subjecting to biaxial stresses at infinity and a uniform normal pressure at the inner cavity wall (i.e. $r = R$). The stress boundaries are expressed in Eqs.(1) and (2). It is assumed that the soil around the cavity is monotonically loaded or unloaded to $-p_{in}$ at the cavity wall with a sufficiently slow speed, deforming under plane strain. For convenience, both Cartesian coordinates (x, y, z) and cylindrical polar coordinates (r, θ, z) are employed.

$$\sigma_r\big|_{r=R} = -p_{in} \tag{1}$$

$$P_\infty = \frac{(\sigma_y\big|_{y\to\infty} + \sigma_x\big|_{x\to\infty})}{2} = -\frac{(\sigma_{v0} + \sigma_{h0})}{2} \ , \ \tau_\infty = \frac{(\sigma_y\big|_{y\to\infty} - \sigma_x\big|_{x\to\infty})}{2} = \frac{(\sigma_{h0} - \sigma_{v0})}{2} \tag{2}$$

For abbreviation, some functions recurring in the derivation process are defined here first.

$$K_p = (1+\sin\varphi)/(1-\sin\varphi)$$

$$Y = 2c\cos\varphi/(1-\sin\varphi)$$

$$\delta = (1-K_p)/(1+K_p)$$

$$S_p = \frac{[(1-K_p)P_\infty + Y]}{K_p+1}$$

where c and φ are effective cohesion and friction angle of the Mohr-Coulomb material respectively.

The surrounding soil is modelled with an elastic-perfectly plastic model. The elastic response is governed by the Hooke's law, and the plastic behaviour is characterised with the Mohr-Coulomb yield criterion as in Eq.(3).

$$K_p\sigma_1 - \sigma_3 = Y \tag{3}$$

where σ_1 and σ_3 are the major and minor principal stress respectively.

ELASTIC AND PLASTIC STRESS ANALYSIS

Owing to the non-hydrostatic far-field stresses, the stress field developed around the inner cavity is no longer axisymmetric, and, therefore, a two-dimensional analysis is necessary. Within the stress range specified by Eq.(4), the surrounding soil deforms purely elastically, and the stresses can be readily calculated with the Kirsch solution (Yu, 2000).

$$-\frac{Y}{K_p+1} - \frac{2}{K_p+1}(P_\infty - 2|\tau_\infty|) \le p_{in} \le \frac{Y}{K_p+1} - \frac{2K_p}{K_p+1}(P_\infty + 2|\tau_\infty|) \tag{4}$$

While plastic yielding occurs, various distributions of the plastic zone may appear, depending on the soil strength and boundary conditions (Bradford and Durban, 1998, Tokar, 1990, Yarushina et al., 2010). As an extension of the Galin's (1946) solution to the Mohr-Coulomb material, the major concern of this note is the distribution of the elastic and plastic stresses around the cavity in the states satisfying two prior assumptions (Detournay, 1986, Yarushina et al., 2010): (1) a plastic zone is developed under pressure, and it is statically determinate, and (2) the inner cavity is fully encircled by the formed plastic zone. These two assumptions confirm the necessity of plastic analysis, theoretically postulate that the plastic stress state is completely determined by the inner stress boundary condition (Hill, 1950), and ensure that the outside elastic field is bounded internally by a closed simple contour (i.e. the elastic-plastic boundary).

Static plastic stress field

According to the above assumptions and the boundary condition of Eq. (1), the radial stress equilibrium equation in the statically determined plastic field can be expressed as

$$\frac{\partial \sigma_r}{\partial r} - \frac{\sigma_\theta - \sigma_r}{r} = 0 \tag{5}$$

where σ_r and σ_θ are the stress components in the radial and circumferential directions respectively. Taking tension as positive, the major principal stress is in the circumferential direction during loading (i.e. $\sigma_\theta > \sigma_r$). On the contrary, the major principal stress orients in the radial direction during unloading (i.e. $\sigma_\theta < \sigma_r$). It is regarded that the axial stress (out-plane direction) always remains as the intermediate stress, which would be satisfied for most of soils (Yu and Houlsby, 1991).

By solving the yield criterion (i.e. Eq.(3)) and equilibrium equation (i.e. Eq.(5)) with the inner stress boundary of Eq.(1), the plastic stresses during both loading and unloading (Yu, 2000) are equal to

$$\sigma_r^p = \frac{Y}{K_p - 1} - (p_{in} + \frac{Y}{K_p - 1})(\frac{r}{R})^{(1/K-1)} \tag{6}$$

$$\sigma_\theta^p = \frac{Y}{K_p - 1} - \frac{1}{K}(p_{in} + \frac{Y}{K_p - 1})(\frac{r}{R})^{(1/K-1)} \tag{7}$$

where $K = K_p$ during loading and $K = 1/K_p$ during unloading.

Conformal mapping function

The elastic-plastic boundary gives the outer boundary of the plastic zone and simultaneously provides the inner boundary for computing the elastic stress field. In general, it is determined by analysing the stress continuity conditions across the interface. The elastic field is not known prior to determining its inner stress and geometry boundary conditions. Alternatively, the elastic stresses are represented by general expressions of the Kolosov-Muskhelishvili complex potentials, $\Phi(\zeta)$ and $\Psi(\zeta)$ (Muskhelishvili, 1963); spatial positions of points in the elastic field are described by a general form of conformal mapping function (Cherepanov, 1963, Detournay, 1986, Galin, 1946). Accordingly, in conjunction with the plastic stress solutions, the continuity conditions of the mean stress and the deviatoric stress along the elastoplastic interface can be expressed as

$$\Phi(\zeta)+\overline{\Phi(\zeta)}=\frac{(\sigma_r+\sigma_\theta)}{2}=\begin{cases}\dfrac{Y}{K_p-1}-S_p\dfrac{(K_p+1)}{(K_p-1)}\left(\dfrac{r}{\chi R}\right)^{(1/K-1)} & ,\text{at } \gamma \quad \text{(a)}\\ P_\infty & ,\zeta\to\infty \quad \text{(b)}\end{cases} \tag{8}$$

$$\frac{\overline{\omega(\zeta)}}{\omega'(\zeta)}\Phi'(\zeta)+\Psi(\zeta)=\frac{(\sigma_\theta-\sigma_r+2i\tau_{r\theta})}{2}e^{-2i\theta}=\begin{cases}\pm S_p\left(\dfrac{r}{\chi R}\right)^{(1/K-1)}\dfrac{\overline{\omega(\sigma)}}{\omega(\sigma)} & ,\text{at } \gamma \quad \text{(a)}\\ \tau_\infty & ,\zeta\to\infty \quad \text{(b)}\end{cases} \tag{9}$$

where $\zeta=\xi+i\eta=\rho e^{i\phi}$, describing the position vectors in the phase plane. $i=\sqrt{-1}$. σ is the complex variable on the unit circle, and $\bar{\sigma}=1/\sigma$. $\omega(\zeta)$ is a function to conformally map the exterior of the elastic-plastic boundary in the physical plane onto the exterior region of the unit circle in the phase plane (represented by γ); $\overline{\omega(\zeta)}$ is its conjugate. The upper signs and lower signs of $\pm$ and $\mp$ (and hereafter) refer to the loading case and the unloading case respectively.

Relying on the Schwarz's reflection principle and Laurent's decomposition theorem, the stress continuity conditions of Eqs.(8) and (9) have been studied by Detournay (1986), and an approximate mapping function in a truncated series form was derived. Numerical computations are required to determine the coefficients of the series by seeking roots of a non-linear system of equations. Alternatively, Detournay (1985) proposed an unified asymptotic mapping function for both loading and unloading analysis as given in Eq.(10).

$$\omega(\zeta)=\alpha\zeta\left(1\pm\frac{\beta}{\zeta^2}\right)^{(1\mp\delta)} \tag{10}$$

where $\alpha=\lambda\chi R$, and $\beta=\tau_\infty/S_p$. In the form of Gaussian hypergeometric function, $\lambda^{1-1/K}={}_2F_1[(\mp\delta,\mp\delta);1,\beta^2]=1+\delta^2\beta^2+0(\beta^4)$.

$$\chi=\left\{\frac{(1+1/K)}{2}\frac{[Y+(K_p-1)p_{in}]}{[Y-(K_p-1)P_\infty]}\right\}^{K/(K-1)} \tag{11}$$

With zero friction angle (i.e. $\varphi=0$), Eq. (10) is the same as the rigorous mapping functions for Tresca materials (Galin, 1946, Yarushina et al., 2010) as $\alpha|_{\varphi=0}=R\exp\left[\dfrac{P_\infty+p_{in}\mp s_u}{\pm 2s_u}\right]$ (s_u represents the undrained shear strength of soil).

It can be found that χ equals the ratio ($\mathrm{r}_{\mathrm{ep}}^{\mathrm{h}} / \mathrm{R}$) of the radius of the circular elastic-plastic boundary to the cavity radius for a cavity expanding (Yu and Houlsby, 1991) or contracting (Yu and Rowe, 1999) within a corresponding uniform initial stress field of P_{∞}. The internal pressure p_{in} enters into the mapping function through the 'scaling' factor χ. Therefore, p_{in} only influences the size of the elastic-plastic boundary in a self-similar manner (Detournay and Fairhurst, 1987). Due to the biaxial far-field stresses, the elastic-plastic boundary is flattened into an oval shape of which the semi-major axis and semi-minor axis equal $[\lambda(1+|\beta|)^{(1\mp\delta)}]\mathrm{r}_{\mathrm{ep}}^{\mathrm{h}}$ and $[\lambda(1-|\beta|)^{(1\mp\delta)}]\mathrm{r}_{\mathrm{ep}}^{\mathrm{h}}$ in length respectively. The long axis of the elastic-plastic boundary is along the direction of the greatest far-field compression stress during loading but along the opposite direction during unloading.

Two-dimensional elastic stress field

The elastic-plastic boundary is given by $\omega(\sigma)$, and stresses along it are known from the plastic stress solution. The elastic stress analysis now becomes a typical stress boundary value problem of determining the Kolosov-Muskhelishvili elastic complex potentials. The infinity values of the complex potentials are specified by the far-field stresses as

$$\Phi(\infty)=\frac{\mathrm{P}_{\infty}}{2}+\mathrm{O}(\zeta^{-2}) \quad , \quad \Psi(\infty)=\tau_{\infty}+\mathrm{O}(\zeta^{-2}) \tag{12}$$

Based on their behaviour at infinity, the Kolosov-Muskhelishvili complex potentials can be expressed in Eqs.(13) and (14) (Muskhelishvili, 1963), in which $\Phi_0(\zeta)$ and $\Psi_0(\zeta)$ are purely holomorphic functions (i.e. $\Phi_0(\infty)=0$; $\Psi_0(\infty)=0$).

$$\Phi(\zeta)=\Phi_0(\zeta)+\frac{\mathrm{P}_{\infty}}{2} \tag{13}$$

$$\Psi(\zeta)=\Psi_0(\zeta)+\tau_{\infty} \tag{14}$$

According to Eqs. (8), (13) and (14), the mean stress continuity condition along the elastic-plastic boundary can be rewritten as

$$\Phi_0(\sigma)+\overline{\Phi_0(\sigma)}=\mathrm{S}_{\mathrm{p}}\frac{(\mathrm{K}_{\mathrm{p}}+1)}{(\mathrm{K}_{\mathrm{p}}-1)}[1-(\frac{\mathrm{r}}{\chi\mathrm{R}})^{(1/\mathrm{K}-1)}] \tag{15}$$

where $(\frac{\mathrm{r}}{\chi\mathrm{R}})^{(1/\mathrm{K}-1)}=\left[\frac{\omega(\sigma)\overline{\omega}(\sigma^{-1})}{(\chi\mathrm{R})^2}\right]^{\frac{(1/\mathrm{K}-1)}{2}}=\lambda^{(1/\mathrm{K}-1)}[(1\pm\beta\sigma^{-2})^{\pm\delta}(1\pm\beta\sigma^{2})^{\pm\delta}]$. By using the binomial expansion formula, terms in this equation can be expressed as

$$(1\pm\beta\sigma^{-2})^{\pm\delta}=\sum_{\mathrm{k}=0}^{\infty}\binom{\pm\delta}{\mathrm{k}}(\pm\beta)^{\mathrm{k}}\sigma^{-2\mathrm{k}}\quad,\quad(1\pm\beta\sigma^{2})^{\pm\delta}=\sum_{\mathrm{k}=0}^{\infty}\binom{\pm\delta}{\mathrm{k}}(\pm\beta)^{\mathrm{k}}\sigma^{2\mathrm{k}} \qquad (16)$$

Accordingly, the right part of Eq.(15) is easy to be split into two functions which are mutual conjugates and analytic in Ω^{+} ($|\zeta|<1$) and Ω^{-} ($|\zeta|>1$) respectively. The parameter λ is determined by the requirement that its zero-order term equals zero. Equation (15) gives the inner boundary value of $\Phi_0(\zeta)$, it therefore can be directly obtained by using the Cauchy integral method as

$$\Phi_0(\zeta)=-\mathrm{S_p}\frac{(\mathrm{K}+1)}{(\mathrm{K}-1)}\sum_{\mathrm{j}=1}^{\infty}\frac{\mathrm{d}_{2\mathrm{j}}}{\zeta^{2\mathrm{j}}} \qquad (17)$$

where $\mathrm{d}_{2\mathrm{j}}=\lambda^{(1/\mathrm{K}-1)}(\pm\beta)^{\mathrm{j}}\binom{\pm\delta}{\mathrm{j}}{}_2\mathrm{F}_1[(\mp\delta,\mp\delta+\mathrm{j});\mathrm{j}+1,\beta^2]$.

The complex potential $\Psi(\zeta)$ is sought by analysing the continuity condition of the deviatoric stress (i.e. Eq.(9)). By multiplying $\frac{1}{2\pi\mathrm{i}}\frac{\mathrm{d}\sigma}{\sigma-\zeta}$ on both sides of Eq.(9) a) and then integrating it along the unit circle in the phase plane from the side of Ω^{-}, $\Psi(\zeta)$ equals

$$\Psi(\zeta)=\pm\mathrm{S_p}\left[\hat{\mathrm{r}}(\zeta)\right]\frac{1}{\zeta^2}\left[\frac{\zeta^2(1\pm\beta\zeta^2)}{\zeta^2\pm\beta}\right]^{1\mp\delta}-\mathrm{M}(\zeta)\Phi'(\zeta)+[1-\lambda^{(1/\mathrm{K}-1)}]\tau_{\infty} \qquad (18)$$

where $\hat{\mathrm{r}}(\zeta)=\lambda^{(1/\mathrm{K}-1)}[1+\beta^2\pm\beta\zeta^2\pm\beta\zeta^{-2}]^{\pm\delta}$. $\mathrm{M}(\zeta)=\frac{1}{\zeta}(\frac{\zeta^2\pm\beta}{\zeta^2\mp\beta+2\beta\delta})[\frac{\zeta^2(1\pm\beta\zeta^2)}{\zeta^2\pm\beta}]^{(1\mp\delta)}$.

The term of $[1-\lambda^{(1/\mathrm{K}-1)}]\tau_{\infty}$ in $\Psi(\zeta)$ is due to the approximation involved by the asymptotic mapping function, and it vanishes when the friction angle gets zero.

Thus far, unified elastic complex potentials for the two-dimensional stress and displacement analysis are derived. The elastic stress components can be computed with

$$\sigma_{\mathrm{x}}^{\mathrm{e}}+\sigma_{\mathrm{y}}^{\mathrm{e}}=4\,\mathrm{Re}[\Phi(\zeta)] \qquad (19)$$

$$\sigma_{\mathrm{y}}^{\mathrm{e}}-\sigma_{\mathrm{x}}^{\mathrm{e}}+2\mathrm{i}\tau_{\mathrm{xy}}^{\mathrm{e}}=2[\frac{\overline{\omega(\zeta)}}{\omega'(\zeta)}\Phi'(\zeta)+\Psi(\zeta)] \qquad (20)$$

DISCUSSION AND SOLUTION VALIDATION

Permissible stress range of rigorous analysis

Two restrictive assumptions were adopted in deriving the analytical solution. They determined that this solution better serves for the cavity analysis in a plane within specific stress states (Detournay, 1986, Yarushina et al., 2010).

The first assumption that the plastic zone is statically determinate requires that points on the cavity rim are connected with the elastic-plastic boundary by two families of characteristic lines, and each characteristic line cuts the elastic-plastic boundary only once (Cherepanov, 1963, Detournay, 1986, Hill, 1950). In this problem, the characteristic lines consist of logarithmic spirals inclined to the radial direction by an angle of $\pi/4-\varphi/2$ during loading and $\pi/4+\varphi/2$ during unloading. The limit condition will be reached while one, and only one, characteristic line is tangent to the elastic-plastic interface within one quadrant. Therefore, this requirement can be expressed as

$$|\lambda-\theta| \le \frac{\pi}{4} \pm \frac{\varphi}{2} \tag{21}$$

$$e^{2i(\lambda-\theta)} = \sigma^2 \frac{\omega'(\sigma)}{\overline{\omega'(\sigma)}} \frac{\overline{\omega(\sigma)}}{\omega(\sigma)} = \frac{(\sigma^2 \mp \beta + 2\beta\delta)(\sigma^{-2} \pm \beta)}{(\sigma^{-2} \mp \beta + 2\beta\delta)(\sigma^2 \pm \beta)} \tag{22}$$

where λ represents the angle between the outward normal to the elastic-plastic interface and the x-axis.

To meet this requirement at any point of the whole plastic zone, the limit condition is only reached at which ($\lambda-\theta$) is extremum (Detournay, 1986). By solving Eqs. (21) and (22) at extremum points, the upper limits of $|\beta|$ can be obtained as shown in Fig.2. With an increasing value of the friction angle, the upper limits decrease in the loading analysis but increase in the unloading analysis. With zero friction angle, the limit value of $|\beta|$ becomes the same during both loading and unloading, which equals $\sqrt{2}-1$, and the same value was also suggested by Detournay (1986) and Yarushina et al. (2010).

The second assumption requires that the cavity is fully enclosed by a connected plastic region. The limit conditions of this restriction will be reached once the elastic-plastic boundary touches the cavity rim at its vertices on the minor axis direction. That is

$$\alpha(1-|\beta|)^{(1\mp\delta)} \ge \mathrm{R} \tag{23}$$

Comparison with other methods

The accuracy of the analytical loading and unloading solutions are validated by comparing with the numerical simulation results computed by the finite element method (FEM) and the solution of Detournay and Fairhurst (1987) respectively. And they are also compared with the Galin's (1946) solution and Yarushina et al.'s (2010) solution in the special cases of infinitesimal friction angle. All the following calculations are conducted within the given admissible application range.

(1) Loading analysis

The numerical simulations are implemented in Abaqus/Standard 6.12 using a quarter model. An 8-node biquadratic plane strain quadrilateral mesh is utilised for meshing. To simulate the far-field stress boundary conditions, the sides of the square model are set as 50 times that of the inner cavity radius. The void ratio of soil is set as 0.4.

In Fig.3, stresses calculated by the present solution closely agree with those by the numerical simulations and Galin's solution (taking φ close to zero). When subjected to non-equal biaxial in-situ stresses, the extent of the plastic region around the inner cavity varies in directions. Plastic tensile failure may first occur in the plane along the maximum far-field compression stress, which is of great interest in estimating the potential failure zone or the initiation pressure of hydrofracturing around an internally pressurised cavity (Guo et al., 2015).

(2) Unloading analysis

As previously introduced, a slight stress discontinuity across the elastic-plastic interface exits in the Detournay and Fairhurst's (1987) unloading solution. Detournay and Fairhurst (1987) pointed out that the level of this discontinuity depends on the far-field stress obliquity ($|\beta|$) and friction angle (φ) and varies in directions. By directly integrating the deviatoric stress continuity condition with the Cauchy integral method, a new expression of the complex potential $\Psi(\zeta)$ for the unloading analysis was given in Eq.(18). These two methods are compared in Fig.4. It is shown that the stress discontinuity phenomenon in the Detournay and Fairhurst's solution is not significant even when $|\beta|$ gets close to its upper limit, and it can be eliminated by the new solution. In the special case of zero friction angle, excellent agreement between the present solution and Yarushina et al.'s (2010) solution is also shown in Fig.5.

(3) Distributions of the plastic zone

It is demonstrated in Figs. 3-6 that accurate predictions of the elastic-plastic boundary can be achieved by the asymptotic-form mapping function of Eq.(10) under both loading and unloading conditions. The distribution of the plastic zone varies with the friction angle, stress boundary conditions, and loading types, and example results are shown in Fig.6.

Figure 6 corroborates that the major axis of the elastic-plastic boundary during loading coincides with the direction of the greatest far-field compression stress whereas it is along the perpendicular direction during unloading. It is shown that the oval-shaped elastic-plastic boundary shrinks with an increasing friction angle in both loading and unloading conditions. While the friction angle is relatively small (e.g. $\varphi \leqslant 15^{o}$ in Fig.6), the frictional strength has a relatively larger influence on the size of the plastic zone. The mapping function of Eq.(10) provides a quick method for predicting the plastically failed zone around an expanding or contracting cavity under biaxial in-situ soil stresses. Example applications of the unloading analysis to predict the size and shape of failed rock regions around a deep tunnel during excavation has been introduced by Detournay and John (1988). Considering the K_0 effect, the loading solution has been successfully applied to predict the peak uplift resistance of shallow strip anchors in sand (Zhuang and Yu, 2018).

CONCLUSIONS

A unified analytical solution was presented for elastic-plastic loading and unloading stress analysis of a cylindrical cavity under biaxial in-situ stresses. The plastic zone was assumed statically determinate and bounded by a continuous elastic-plastic boundary. As a result, the adopted assumptions specified an admissible application range of this solution, which was found mainly determined by the far-field stress obliquity, soil strength and loading type. In the admissible application range, the elastic-plastic boundary was described by an asymptotic conformal mapping function, which is in oval-shape in Mohr-Coulomb materials under biaxial far-field stresses. It was found that the major axis of the elastic-plastic boundary coincides with the direction of the greatest far-field compression stress during loading whereas it is along the perpendicular direction during unloading. By comparing with FEM simulations and other analytical solutions, it was demonstrated that accurate results can be obtained by the new analytical solution.

ACKNOWLEDGEMENTS

The authors thank one of the anonymous reviewer for providing the reference of Detournay (1985). The present work was partly conducted at the Nottingham Centre for Geomechanics (NCG). The first author would like to acknowledge the financial supports provided by the University of Nottingham and the China Scholarship Council for his PhD study.

REFERENCES

Bishop, R. F., Hill, R. & Mott, N. F. (1945). The theory of indentation and hardness tests. The proceedings of the Physical Society 57, **No**. 3, 147–159.

Bradford, I. D. R. & Durban, D. (1998). Stress and deformation fields around a cylindrical cavity embedded in a pressure-sensitive elastoplastic medium. Journal of Applied Mechanics 65, **No**. 2, 374-379.

Carranza-Torres, C. & Fairhurst, C. (2000). Application of the convergence-confinement method of tunnel design to rock masses that satisfy the Hoek-Brown failure criterion. Tunnelling and underground space Technology 15, **No**. 2, 187-213.

Cherepanov, G. P. (1963). On a method of solving the elasto-plastic problem. Journal of Applied Mathematics and Mechanics 27, **No**. 3, 644-655.

Detournay, E. (1985). Solution approximative de la zone plastique autour d'une galerie souterraine soumise a un champ de contrainte non hydrostatique. In Comptes Rendus-Academie des Sciences Serie II, 12 edn. vol. 301, pp. 857-860 (in French).

Detournay, E. (1986). An approximate statical solution of the elastoplastic interface for the problem of Galin with a cohesive-frictional material. International Journal of Solids and Structures 22, **No**. 12, 1435-1454.

Detournay, E. & Fairhurst, C. (1987). Two-dimensional elastoplastic analysis of a long, cylindrical cavity under non-hydrostatic loading. International Journal of Rock Mechanics and Mining Sciences & Geomechanics Abstracts 24, **No**. 4, 197-211.

Detournay, E. & John, C. M. S. (1988). Design charts for a deep circular tunnel under non-uniform loading. Rock Mechanics and Rock Engineering 21, **No**. 2,119-137.

Galin, L. A. (1946). Plane elastic-plastic problem: plastic regions around circular holes in plates and beams. Prikladnaia Matematika i Mekhanika 10, 365-386.

Gao, X. L., Wei, X. X. & Wang, Z. K. (1991). A general analytical solution of a strain-hardening elasto-plastic plate containing a circular hole subjected to biaxial loading-with applications in pressure vessels. International journal of pressure vessels and piping 47, **No**. 1, 35-55.

Guo, J., He, S., Deng, Y. & Zhao, Z. (2015). New stress and initiation model of hydraulic fracturing based on nonlinear constitutive equation. Journal of Natural Gas Science and Engineering 27, 666-675.

Guo, P. (2010). Effect of density and compressibility on K_0 of cohesionless soils. Acta Geotechnica 5, **No**. 4, 225-238.

Henrici, P. (1993). Applied and Computational Complex Analysis. Volume 3 Discrete Fourier Analysis, Cauchy integrals, Construction of Conformal Maps, Univalent Functions. New York: John Wiley & Sons.

Hill, R. (1950). The mathematical theory of plasticity. London: Oxford University Press.

Hu, N., Shang, X.-Y. & Yu, H.-S. (2017). Theoretical Analysis of Pressure-Dependent K_0 for Normally Consolidated Clays Using Critical State Soil Models. International Journal of Geomechanics 18, **No**. 3, 04017159.

Lee, J., Yun, T. S., Lee, D. & Lee, J. (2013). Assessment of K0 correlation to strength for granular materials. Soils and Foundations 53, **No**. 4, 584-595.

Lee, Y. S. & Gong, H. (1987). Application of complex variables and pseudo-stress function to power-law materials and stress analysis of single rigid inclusion in power-law materials subjected to simple tension and pure shear. International Journal of Mechanical Sciences 29, **No**. 10, 669-694.

Mayne, P. W. & Kulhawy, F. H. (1982). K_0- OCR Relationships in Soil. Journal of the Soil Mechanics and foundations Division 108, **No**. 6, 851-872.

Mo, P. Q. & Yu, H. S. (2017). Undrained Cavity-Contraction Analysis for Prediction of Soil Behavior around Tunnels. International Journal of Geomechanics 17, **No**. 5, 1-10 (04016121).

Muskhelishvili, N. I. (1963). Some basic problems of the mathematical theory of elasticity, 4th edn. Groningen, the Netherlands.: P. Noordhoff.

Panah, A. K. & Yanagisawa, E. (1989). Laboratory studies on hydraulic fracturing criteria in soil. Soils and Foundations 29, **No**. 4, 14-22.

Parasyuk, O. S. (1948). An elastic-plastic problem with a non-biharmonic plastic state. Prikladnaya Matematika i Mekhanika 13, 367-370.

Rostami, A., Yi, Y. & Bayat, A. (2016). Estimation of Maximum Annular Pressure during HDD in Noncohesive Soils. International Journal of Geomechanics 17, **No**. 4, 06016029.

Savin, G. N. (1970). Stress distribution around holes. Washington, D.C.: National Aeronautics and Space Administration.

Staheli, K., Bennett, D., O'donnell, H. W. & Hurley, T. J. (1998). Installation of pipeline beneath levees using horizontal directional drilling (Technical Report CPAR-GL-98-1). US Army Corps of Engineers, Vicksburg, MS, USA.

Timoshenko, S. P. & Goodier, J. N. (1951). Theory of elasticity, 2nd edn. New York, USA: McGraw-Hill.

Tokar, G. (1990). Generalization of Galin's problem to frictional materials and discontinuous stress fields. International Journal of Solids and Structures 26, **No**. 2, 129-147.

Vesic, A. S. (1971). Breakout resistance of objects embedded in ocean bottom. Journal of the Soil Mechanics and foundations Division 97, **No**. 9, 1183-1205.

Xia, H. W. & Moore, I. D. (2006). Estimation of maximum mud pressure in purely cohesive material during directional drilling. Geomechanics and Geoengineering: An International Journal 1, **No**. 1, 3-11.

Yanagisawa, E. & Panah, A. K. (1994). Two dimensional study of hydraulic fracturing criteria in cohesive soils. Soils and Foundations 34, **No**. 1, 1-9.

Yarushina, V. M., Dabrowski, M. & Podladchikov, Y. Y. (2010). An analytical benchmark with combined pressure and shear loading for elastoplastic numerical models. Geochemistry, Geophysics, Geosystems 11, **No**. 8, 1-16.

Yu, H. S. (2000). Cavity expansion methods in geomechanics. The Netherlands: Kluwer Academic Publishers.

Yu, H. S. & Houlsby, G. T. (1991). Finite cavity expansion in dilatant soils: loading analysis. Geotechnique 41, **No**. 2, 173-183.

Yu, H. S. & Houlsby, G. T. (1995). A large strain analytical solution for cavity contraction in dilatant soils. International Journal for Numerical and Analytical Methods in Geomechanics 19, **No**. 11, 793-811.

Yu, H. S. & Rowe, R. K. (1999). Plasticity solutions for soil behaviour around contracting cavities and tunnels. International Journal for Numerical and Analytical Methods in Geomechanics 23, **No**. 12, 1245-1279.

Zhuang, P. & Yu, H. S. (2018). Uplift resistance of horizontal strip anchors in sand: a cavity expansion approach. Geotechnique letters. Under review.

Figures

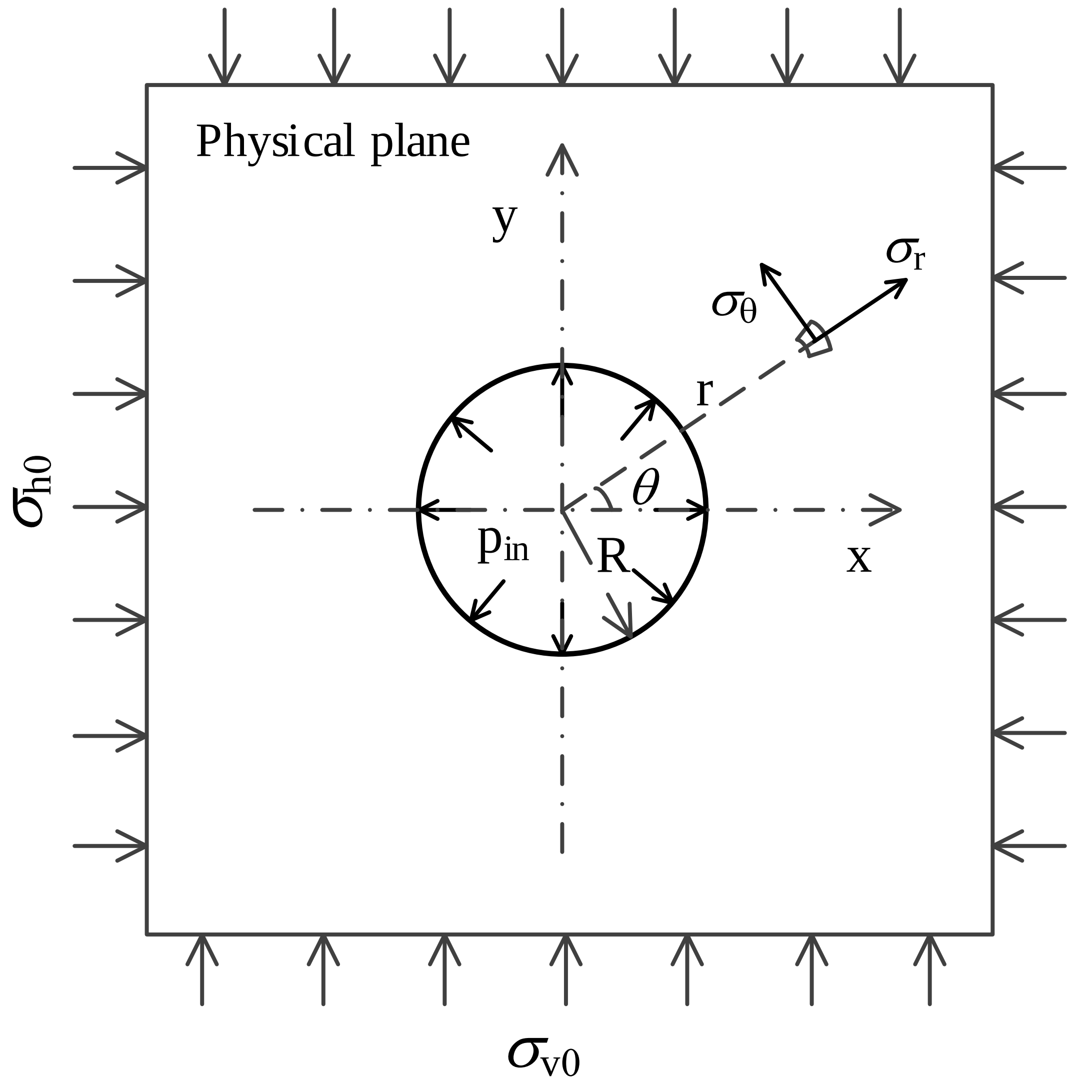

Fig.1 Coordinate systems and stress boundary conditions

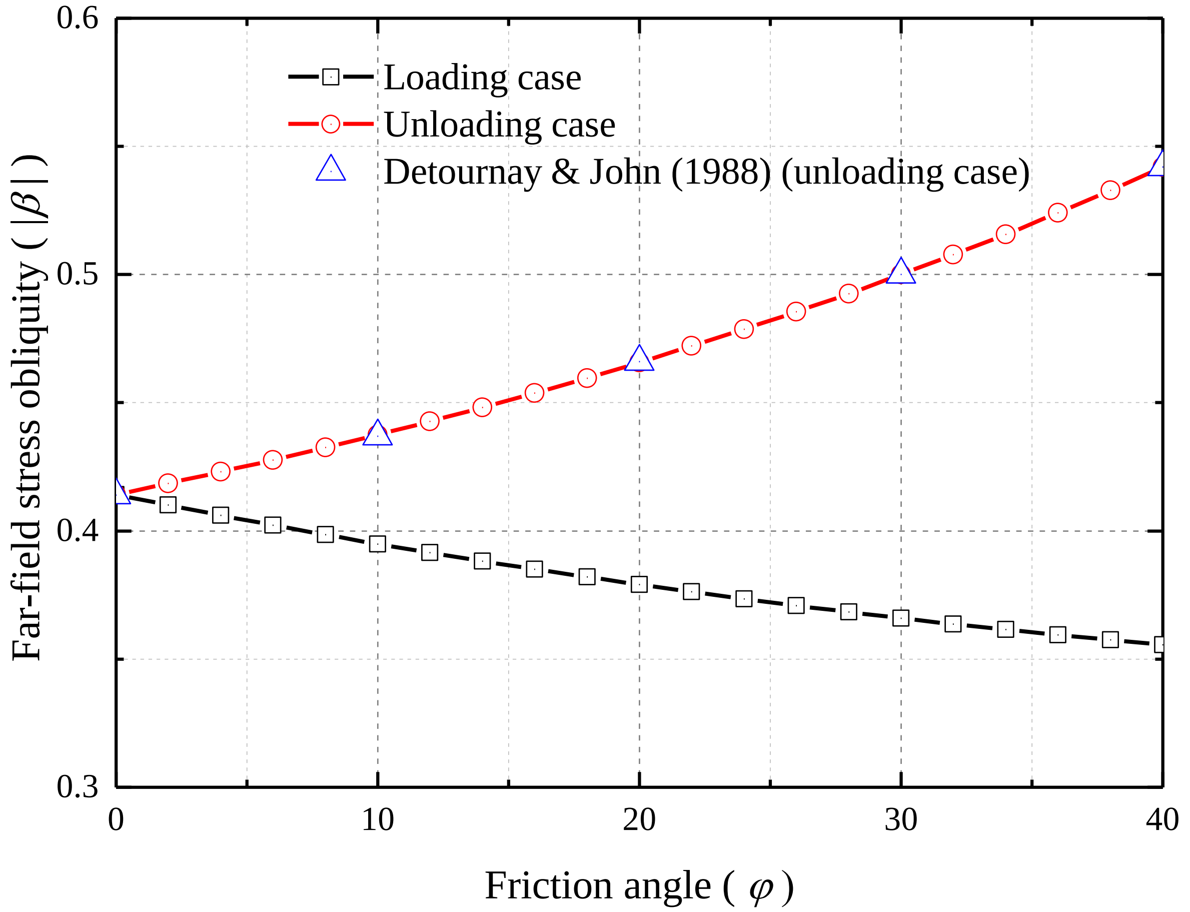

Fig.2 Upper limits of the far-field stress obliquity varying with friction angle

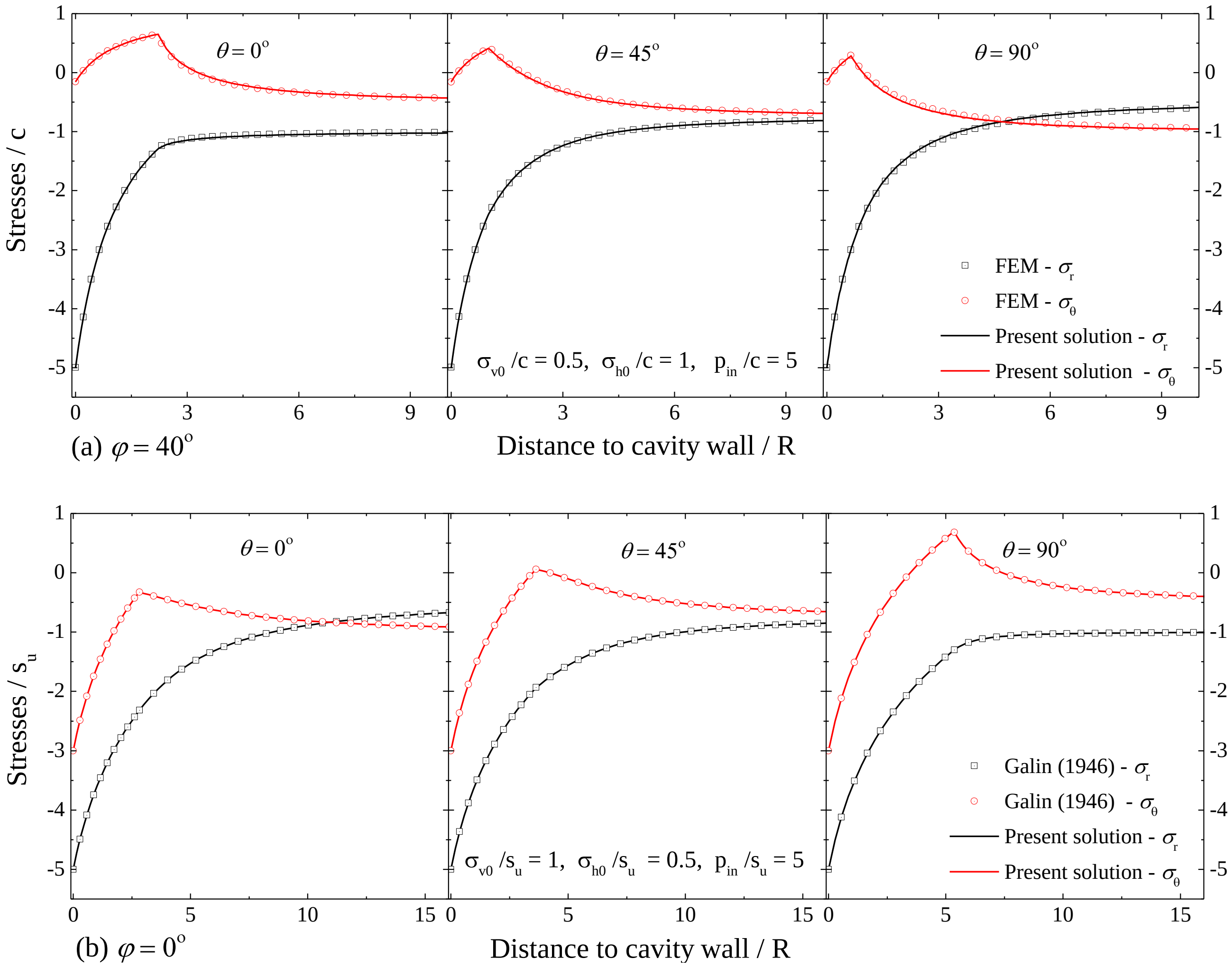

Fig.3 Comparison of stress distribution along different directions (loading case): (a) with FEM results; (b) with Galin's (1946) solution

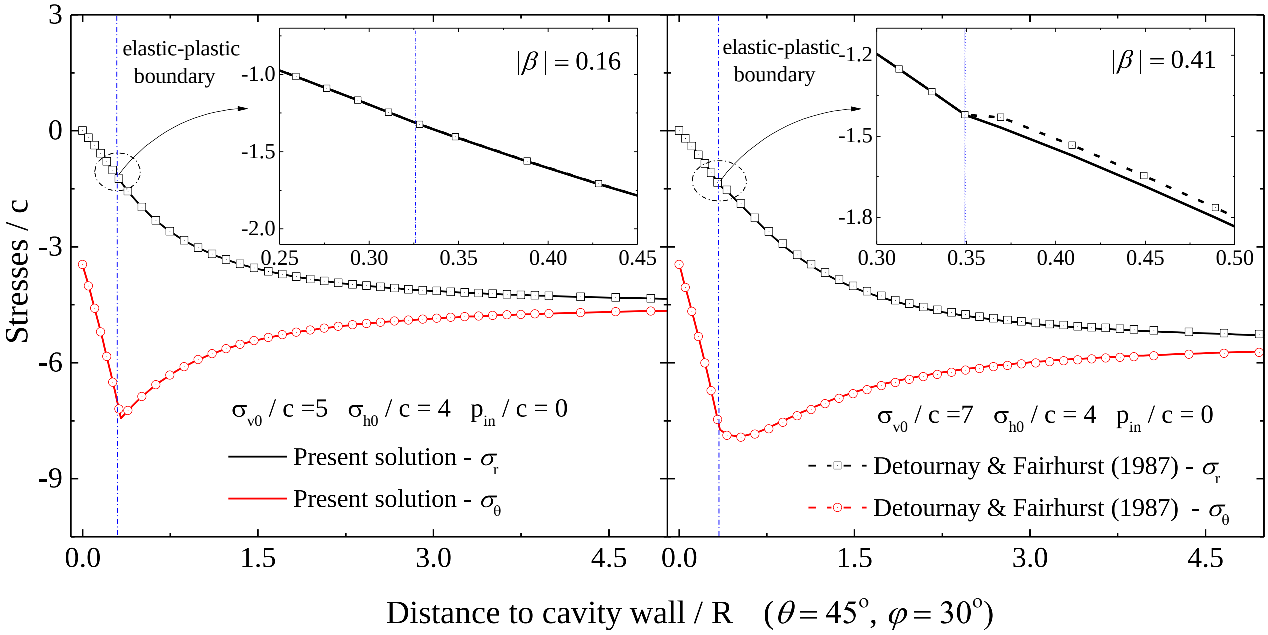

Fig.4 Comparison with Detournay and Fairhurst's solution (1987) (unloading)

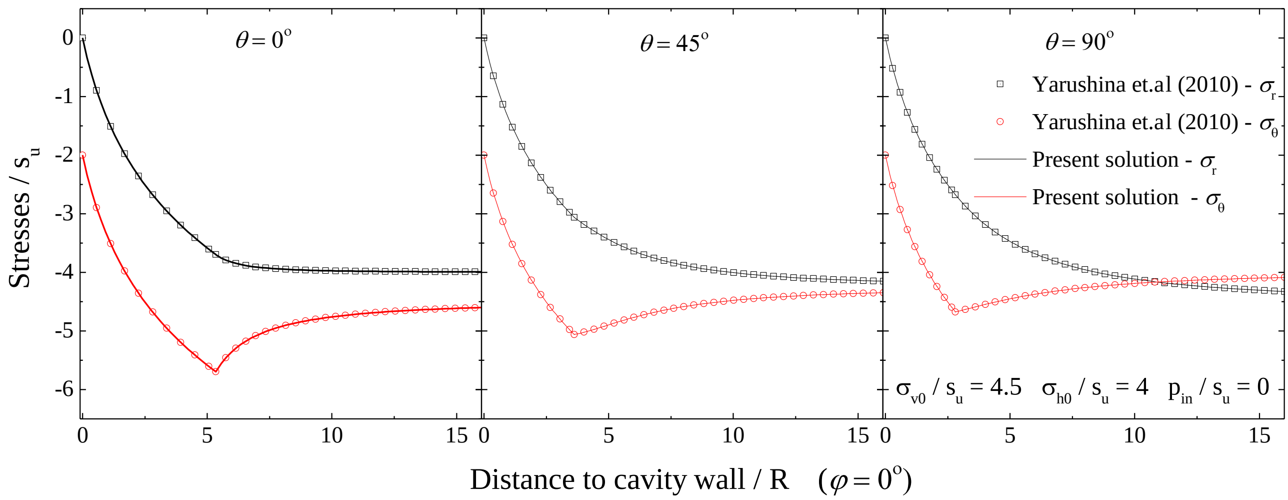

Fig.5 Comparison of unloading stress solutions in a frictionless material

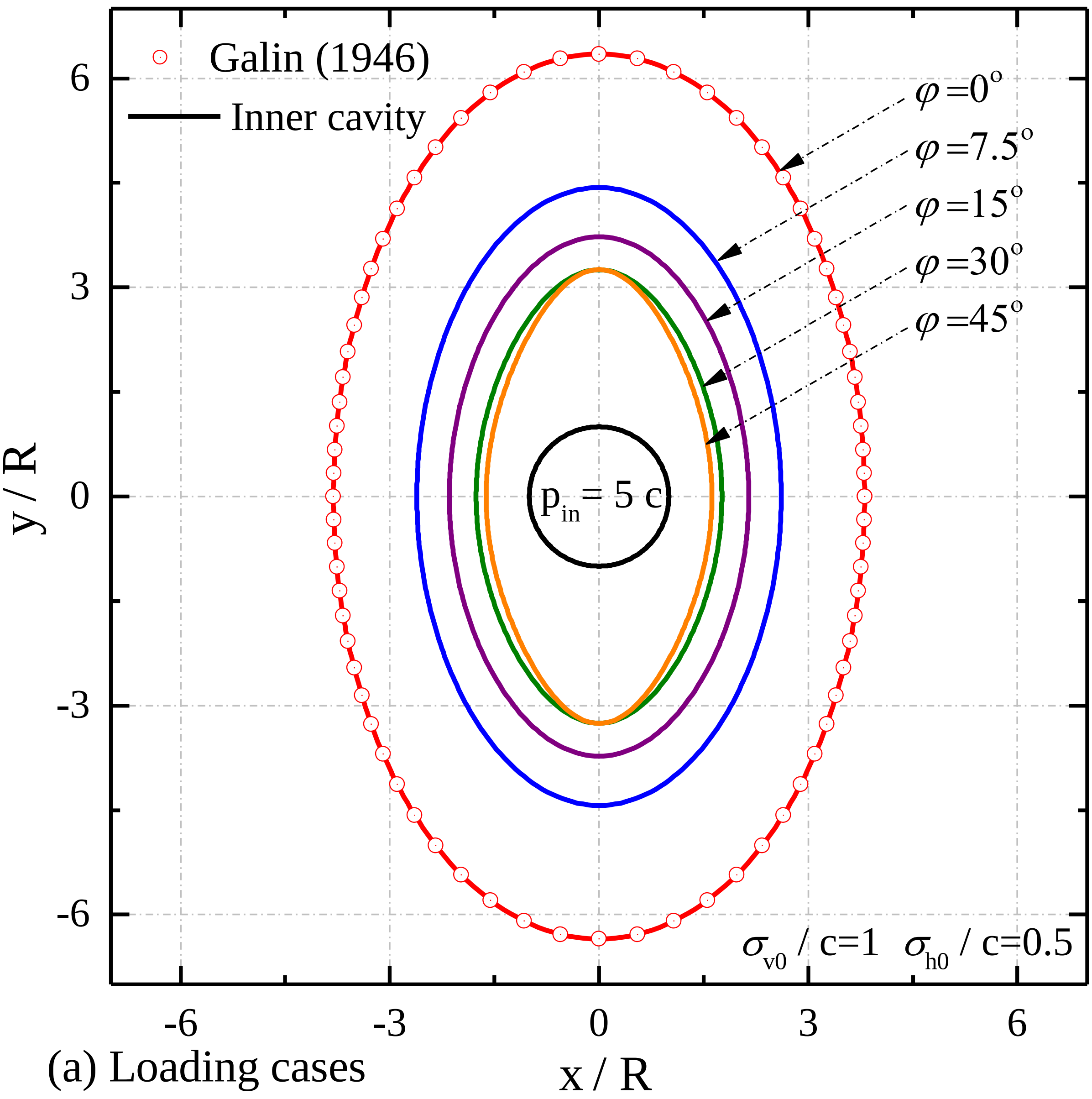

(a) Loading cases

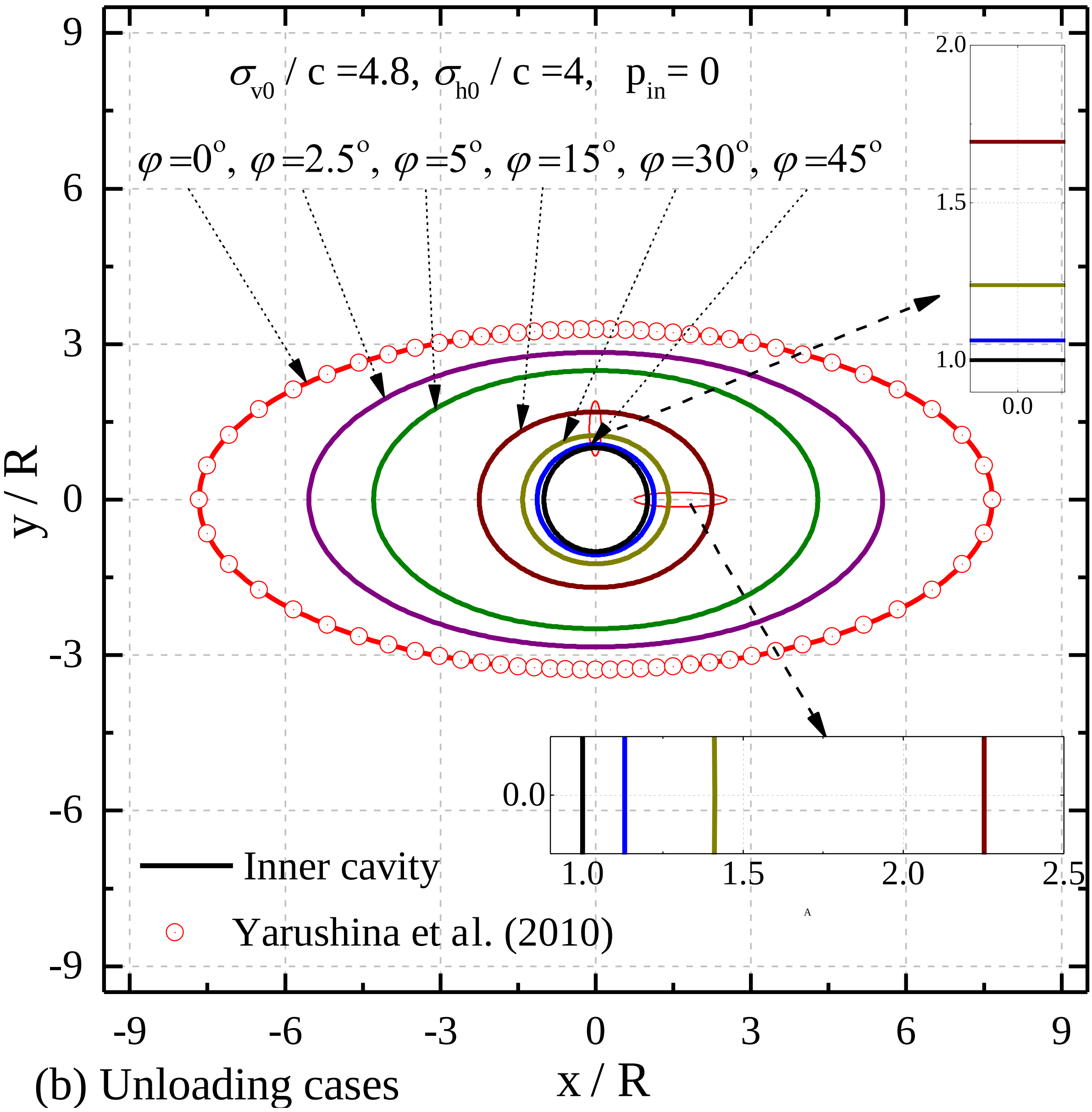

(b) Unloading cases

Fig.6 Elastic-plastic boundary varying with friction angles: (a) loading analysis; (b) unloading analysis